

Numerical Accuracy Matters: Applications of Machine Learned Potential Energy Surfaces

Silvan Käser and Markus Meuwly*

Department of Chemistry, University of Basel, Klingelbergstrasse 80 , CH-4056 Basel, Switzerland.

E-mail: m.meuwly@unibas.ch

November 30, 2023

Abstract

The role of numerical accuracy in training and evaluating neural network-based potential energy surfaces is examined for different experimental observables. For observables that require third- and fourth-order derivatives of the total energy with respect to Cartesian coordinates single-precision arithmetics as is typically used in ML-based approaches is insufficient and leads to roughness of the underlying PES as is explicitly demonstrated. Increasing the numerical accuracy to double-precision yields a smooth PES with higher-order derivatives that are numerically stable and yield meaningful anharmonic frequencies and tunneling splitting as is demonstrated for H₂CO and malonaldehyde. For molecular dynamics simulations, which only require first-order derivatives, single-precision arithmetics appears to be sufficient, though.

Traditional machine learning frameworks/models operate at 32-bit (single precision) to reduce the computational cost for training and inference and for memory efficiency. Much of this appears to be driven by the notion that minimizing the loss function does not benefit from increased accuracy. The performance of approximate, non-deterministic computations in the context of neural network optimization and inference was tested for deep and convolutional neural networks for which the MNIST¹ (handwriting) and CIFAR10² (image classification) datasets were used.³ For such applications it was found that the noise-tolerance of neural networks combined with stochastic rounding during training lead to results close to 32-bit computations. More recently, even further reduced floating point precision, such as half precision (16-bit), has been used.^{3,4} It should be noted that in these and more recent computations for large language models typically only first derivatives are required.^{5,6} However, there may be advantages in or even requirements for increased accuracy at the inference step depending on the application considered, such as in the natural sciences.

One of the recent successful applications of machine learning in molecular sciences is the construction of neural network-based potential energy surfaces (PESs). The ability to conceive full-dimensional PESs for molecules has revolutionised the field of molecular simulations.⁷⁻¹¹ This is primarily due to their ease-of-use and versatility. Also, they have shown to reproduce the input data quite accurately, with representation errors well below chemical accuracy (1 kcal/mol). On the other hand, compared with empirical energy functions, the number of floating-point operations (FLOPS) for evaluating one energy and the forces even for a small molecule can be large. For example, the neural network underlying PhysNet¹² contains of the order of 10^6 learnable parameters. This is based on a feature vector of size 10^2 (128) per atom which leads to $10^2 \times 10^2$ FLOPS for each matrix-vector multiplication (MVM). There are ~ 10 MVMs per module. For a network with 5 modules and for a molecule with 10 atoms this yields $\sim 10^9$ FLOPS if application of the activation functions is also accounted for. This estimate does not yet include initialization and computation of the radial basis

functions.

The precision with which these numerical operations are carried out during inference is decisive for the accuracy of one evaluation (e.g. the energy or the forces) of the neural network. While for many practical applications in atomistic simulations inaccuracies in the total energy on the order of $\sim 10^{-5}$ kcal/mol remain without consequences, depending on the observable of interest the accuracy with which such calculations are carried out will be important. This is considered in the present contribution for a perturbative treatment of the molecular vibrations and tunneling splittings of medium-sized molecules.

The present contribution examines and quantifies how two NN-PESs based on the PhysNet¹² architecture perform depending on whether 32-bit (NN^{F32}) or 64-bit (NN^{F64}) arithmetics is used for training and evaluation. The systems considered are (an)harmonic vibrations of formaldehyde (H_2CO) and tunneling splittings for hydrogen transfer in malonaldehyde $\text{HO}(\text{CH})_3\text{O}$.

The reference data (E , \mathbf{F} , $\boldsymbol{\mu}$) for the H_2CO PESs was determined at the MP2/aug-cc-pVTZ level of theory.¹³ The data set contains a total of 3601 structures for H_2CO obtained from normal mode sampling.¹⁴ For training, the 3601 structures were split into training/validation/test sets according to 3061/360/180 and the training was repeated twice on different splits of the data. After initialization, the parameters of the NN are optimized by minimizing a loss function using ADAM¹⁵ with a learning rate of 10^{-3} and a batch size of 32 randomly chosen structures. For malonaldehyde reference data at the MP2/aug-cc-pVTZ (low-level, LL) and CCSD(T)/aug-cc-pVTZ (high-level, HL) levels of theory are available from which PESs are trained.¹⁶ First, a LL representation of the PES is obtained from ~ 70000 data points, which is then transfer learned (TL) to the CCSD(T)/aug-cc-pVTZ level using the 862 configurations with corresponding E , \mathbf{F} , $\boldsymbol{\mu}$.¹⁶ For the NN^{F32} and NN^{F64}

models everything except the floating-point precision was kept unchanged.

Table 1: Comparison of the test set errors for a total of 4 PhysNet-based NN potentials for H₂CO. Two models operate at single- (NN_{*i*}^{F32}) and two at double-precision (NN_{*i*}^{F64}). The NN_{*i*}^{F64} models reach energy errors that are two orders of magnitude lower, while the effect on the forces is less pronounced but clearly visible.

	NN ₁ ^{F32}	NN ₂ ^{F32}	NN ₁ ^{F64}	NN ₂ ^{F64}
MAE (<i>E</i>) kcal/mol	7.2E-3	1.3E-3	1.6E-5	1.0E-5
RMSE (<i>E</i>)kcal/mol	7.2E-3	1.3E-3	4.6E-5	1.5E-5
MAE (<i>F</i>) kcal/mol/Å	1.4E-3	1.4E-3	5.0E-4	2.8E-4
RMSE (<i>F</i>)kcal/mol/Å	3.7E-3	3.4E-3	3.0E-3	6.0E-4

The test set errors for all four PhysNet models for H₂CO are listed in Table 1. NN^{F32} reaches out of sample MAE(*E*) of several 10⁻³ kcal/mol while for NN^{F64} the energy errors are reduced by two orders of magnitude. For the forces, NN^{F64} reduces the error to several 10⁻⁴ kcal/mol/Å and lower, whereas NN^{F32} remains consistently above 10⁻³ kcal/mol/Å. For the following analysis, the two models with lower out-of-sample errors are used (*i.e.*, NN₂^{F32} and NN₂^{F64}).

Harmonic frequencies ω , from diagonalising the mass-weighted Hessian matrix, were determined with both NN₂^{F32} and NN₂^{F64} and compared with *ab initio* MP2/aug-cc-pVTZ frequencies together with their absolute deviations in Table 2. All computed harmonic frequencies are within 0.2 cm⁻¹ from their reference and illustrate the high quality of the NN-PESs around the minimum. While both floating-point variants reach similar deviations with respect to the reference harmonic frequencies with MAE(ω) of 0.08 and 0.05 cm⁻¹, respectively, NN₂^{F64} is consistently more accurate.

A widely used improvement of harmonic frequencies to include effects of mechanical anharmonicity is to determine perturbative corrections up to second order (VPT2).¹⁷ Such calculations require third- and fourth-order derivatives of the energy with respect to nuclear

Table 2: Harmonic frequencies determined by diagonalising the mass-weighted Hessian matrix and VPT2 frequencies as obtained from NN_2^{F32} and NN_2^{F64} . All values are given in cm^{-1} . The frequencies are compared to their *ab initio* MP2/aug-cc-pVTZ level reference and the absolute difference $|\Delta|$ is shown. Both NN potentials yield harmonic frequencies of similar quality which do not exceed an absolute error of 0.2 cm^{-1} , although NN_2^{F64} reaches lower errors on average.

Harm.	NN_2^{F32}	$ \Delta $	NN_2^{F64}	$ \Delta $	MP2 Ref.
1	1196.65	0.01	1196.66	0.00	1196.66
2	1266.70	0.03	1266.73	0.00	1266.73
3	1539.91	0.03	1539.96	0.02	1539.94
4	1752.47	0.10	1752.41	0.04	1752.37
5	2973.11	0.12	2973.12	0.11	2973.23
6	3047.10	0.18	3047.14	0.14	3047.28
MAE		0.08		0.05	
VPT2	NN_2^{F32}	$ \Delta $	NN_2^{F64}	$ \Delta $	MP2 Ref.
1	1179.94	0.29	1180.19	0.05	1180.23
2	1246.67	0.05	1246.65	0.06	1246.72
3	1507.47	0.48	1507.48	0.47	1507.95
4	1716.10	4.84	1718.81	2.13	1720.94
5	2823.11	3.55	2825.09	1.58	2826.67
6	2859.67	2.94	2860.78	1.83	2862.61
MAE		2.02		1.02	

positions which need to be carried out numerically. If carried out within the realm of *ab initio* calculations this leads to prohibitively long computation times for all but the smallest molecules and at sufficiently high levels of quantum chemical theory. Recently, a viable alternative combining ML-based PESs and TL demonstrated that VPT2 calculations at the CCSD(T) level are possible for molecules the size of CH_3CONH_2 .¹³ The VPT2 frequencies using $\text{NN}_2^{\text{F}32}$ and $\text{NN}_2^{\text{F}64}$ for H_2CO are given in Table 2 and are compared with *ab initio*-calculated values at the MP2/aug-cc-pVTZ level of theory. While both model types perform reasonably well, the prediction error of $\text{NN}_2^{\text{F}32}$ is now often larger by a factor of two or more compared to $\text{NN}_2^{\text{F}64}$. The average difference for $\text{NN}_2^{\text{F}32}$ and $\text{NN}_2^{\text{F}64}$ is 2 cm^{-1} and 1 cm^{-1} , respectively.

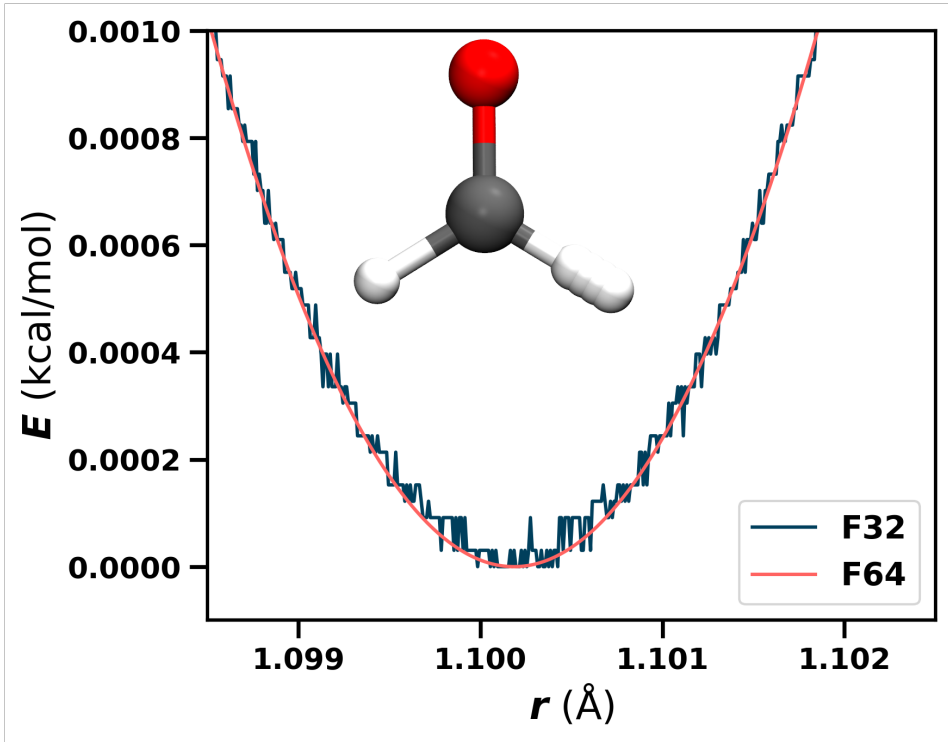


Figure 1: High-resolution potential energy scan along a C–H bond of H_2CO with both $\text{NN}_2^{\text{F}32}$ and $\text{NN}_2^{\text{F}64}$. The scan has been recorded with a step size of $\Delta r = 0.00001 \text{ \AA}$ and only shows the region in the vicinity of the global minimum. From the potential energy scan, it is obvious that the $\text{NN}_2^{\text{F}32}$ PES has a higher “roughness” and its effect on computable observables remains to be clarified.

The most likely reason for the differences between $\text{NN}_2^{\text{F}32}$ and $\text{NN}_2^{\text{F}64}$ are inaccuracies in the numerical derivatives due to small-scale variations of the underlying PES, *i.e.*, due to “roughness” of the PES. In order to test this hypothesis, the two PESs were scanned along a representative coordinate, which was the C–H bond and using a small step size of $\Delta r = 10^{-5}$ Å. The resulting energy scans around the minimum energy structure are shown in Figure 1. It is obvious that the $\text{NN}_2^{\text{F}32}$ PES reveals small-scale energy variations (10^{-5} kcal/mol) whereas for $\text{NN}_2^{\text{F}64}$ the PES remains smooth viewed on the same energy scale. Given that the harmonic frequencies are rather insensitive to whether $\text{NN}_2^{\text{F}32}$ or $\text{NN}_2^{\text{F}64}$ is used, but more pronounced differences arise if higher-order derivatives are required as for VPT2 calculations, it is conceivable that “roughness” which is present for $\text{NN}_2^{\text{F}32}$ but not for $\text{NN}_2^{\text{F}64}$ has a detrimental effect on performance.

One possibility to *quantify* roughness of a PES can be based on concepts from atomic force microscopy.^{18,19} Given a height profile z measured using an atomic force microscope, the roughness can be characterised in terms of the root mean squared roughness given by

$$R_{\text{rms}} = \sqrt{\frac{1}{N} \sum_{i=1}^N |z_i^2|}. \quad (1)$$

Here, N corresponds to the number of data points or “measurements” and z_i is the deviation of the measurement i from a n –point average. For the $\text{NN}_2^{\text{F}32}$ and $\text{NN}_2^{\text{F}64}$ PESs first a smoothed PES was determined from a 5-point moving average. Next, R_{rms} was calculated, which yields $R_{\text{rms}} = 2 \cdot 10^{-5}$ and $R_{\text{rms}} = 7 \cdot 10^{-8}$ kcal/mol for $\text{NN}_2^{\text{F}32}$ and $\text{NN}_2^{\text{F}64}$, respectively. For $\text{NN}_2^{\text{F}32}$ this corresponds approximately to the magnitude of the variations in Figure 1. It should be noted that R_{rms} allows to quantify the roughness of a PES, but its magnitude depends on the scanning step size and the window used for computing the running average.

For malonaldehyde, the $\text{NN}^{\text{F}32}$ and $\text{NN}^{\text{F}64}$ PESs were used to obtain tunneling splittings

from ring polymer instanton (RPI) calculations.²⁰ Consistent with previous work¹⁶ that reported $\sim 25 \text{ cm}^{-1}$, the NN^{F32} and NN^{F64} PESs yield tunneling splittings of 25.3 cm^{-1} and 24.2 cm^{-1} , compared with 21.6 cm^{-1} from experiment.²¹ Depending on the coordinate system used, fixed-node Diffusion Monte Carlo (DMC) simulations on a PES based on near-basis-set-limit frozen-core CCSD(T) electronic energies and represented as permutationally invariant polynomials (PIPs) find $21.6 \pm 3 \text{ cm}^{-1}$ and $22.6 \pm 3 \text{ cm}^{-1}$.²² Using the same PES, RPI simulations reported 25 cm^{-1} .²³

Table 3: Multiplicative correction factors c_{CF} to RPI tunneling splittings Δ_{RPI} , which are obtained with two different step sizes for numerical differentiation. The correction factors are obtained for both NN^{F32} and NN^{F64} and the perturbatively corrected tunneling splittings are calculated as $\Delta_{\text{RPI+PC}} = c_{\text{CF}} \cdot \Delta_{\text{RPI}}$. While c_{CF} is consistent across different steps sizes for NN^{F64} , large differences are found for NN^{F32} . The experimentally reported tunneling splitting for H-transfer is $\Delta_{\text{Exp.}} = 21.6 \text{ cm}^{-1}$.^{21,24}

step size		$\Delta_{\text{RPI}} (\text{cm}^{-1})$	c_{CF}	$\Delta_{\text{RPI+PC}} (\text{cm}^{-1})$
0.001	NN^{F32}	25.3	8.91	225.4
	NN^{F64}	24.2	0.91	22.1
0.0005	NN^{F32}	25.3	21.74	550.0
	NN^{F64}	24.2	0.91	22.1

Recently, a perturbative correction for RPI simulations was presented which determines a multiplicative factor c_{CF} to account for anharmonic effects and intermode coupling.²⁵ Computation of c_{CF} requires third- and fourth-order derivatives of the total energy with respect to Cartesian coordinates which need to be carried out numerically, similar to the situation for VPT2 calculations. The corrections c_{CF} to the RPI splittings for different step sizes in the numerical differentiation and for both PESs are listed in Table 3. For NN^{F64} the correction is $c_{\text{CF}} = 0.91$ irrespective of step size and yields a corrected tunneling splitting of 22.1 cm^{-1} which is in excellent agreement with the experimental value of 21.6 cm^{-1} .^{21,24} Contrary to that, the “correction”, which is expected to be ~ 1 , ranges from 8.9 to 21.7 depending on the step size when using NN^{F32} . Hence, the roughness of NN^{F32} (see below) has a detrimental

effect for higher-order derivatives which renders the perturbative corrections to RPI meaningless. Finally, using a semi-global PES,²⁶ very recent RPI+PC simulations also found 22.1 cm^{-1} .²⁵

The roughness of the two PESs for malonaldehyde, NN^{F32} and NN^{F64} , was also assessed by computing R_{rms} along a C-H bond. Maintaining the same parameters (*i.e.*, step size of $\Delta r = 10^{-5}$ Å for scanning the potential energy and a window of $n = 5$ for the running average) as for H_2CO , the roughness for the NN^{F32} and NN^{F64} PESs for malonaldehyde are $5 \cdot 10^{-5}$ and $8 \cdot 10^{-8}$ kcal/mol, respectively. Therefore, for NN^{F32} the roughness increases by a factor of 2.5 compared with NN^{F32} for H_2CO whereas that for NN^{F64} remains almost unchanged for the two molecules. It is interesting to note that for NN^{F32} the increase in roughness and size in going from H_2CO to $\text{C}_3\text{H}_4\text{O}_2$ is comparable.

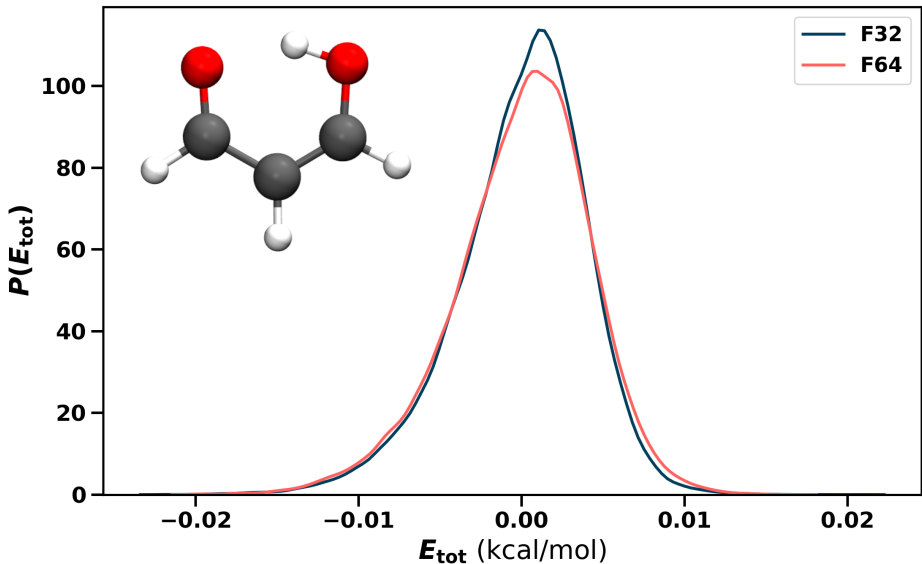


Figure 2: Energy conservation for constant- NVE simulations run at 500 K with both NN^{F32} and NN^{F64} . A time step of 0.25 fs and the Velocity Verlet integrator²⁷ as implemented in ASE²⁸ were used. The total simulation time was 0.5 ns. Herein, the mean of E_{tot} is shifted to zero. The slight asymmetry in $P(E_{\text{tot}})$ may be due to the fact that the dynamics is not fully equilibrated with respect to hydrogen transfer.

An important application of NN-based PESs is their use in atomistic simulations, specifically

molecular dynamics (MD) simulations.^{29–31} Therefore, energy conservation in gas-phase simulations was also assessed in constant- NVE simulations for malonaldehyde using the NN^{F32} and NN^{F64} PESs. For this, the total energy time series $E(t)$ was recorded from 0.5 ns simulations with a time step of $\Delta t = 0.25$ fs using the Velocity Verlet algorithm²⁷ as implemented in ASE.²⁸ Initially, the system was heated to 500 K. The histograms $P(E)$, reported in Figure 2, are near-Gaussian with a standard deviation of ~ 0.004 kcal/mol, for both PESs NN^{F32} and NN^{F64} . Hence, the roughness in NN^{F32} does not have deteriorating effects when used in NVE simulations.

The effects of single- and double-precision arithmetics was studied previously for integrators of the equations of motion used in MD simulations.³² In a dedicated study the degree to which total energy was not conserved in NVE simulations was found to also depend on the numerical accuracy used. Accumulation of errors led simulations carried out with single-precision arithmetics using the GROMACS MD code to severely violate the conservation of total energy whereas changing to double-precision arithmetics conserved this quantity on the nanosecond time scale for an extended system. Interestingly, it was also possible to formulate a correction scheme for integrating the equations of motion that conserved E even within single-precision arithmetics.

The increased sensitivity of the gradients and higher-order derivatives to the roughness of the PES is reminiscent of approximate correlated *ab initio* methods such as local MP2.³³ Truncations by neglecting matrix elements below a certain magnitude, in order to speed up the calculations, lead to numerical precision issues for gradients and, even more acutely, for second derivatives.³⁴

Using double-precision arithmetics in the present case leads to long training times (several weeks compared to days for H_2CO) and evaluation times increase by 30 to 40 %. It is

concluded that depending on the application, double-precision accuracy in training and evaluating NN-based PESs is mandatory. On the other hand, for MD studies, single-precision numerics is likely to be sufficient for meaningful simulations.

This work provides a critical assessment of the influence of floating-point precision within the context of NN-based PESs. The findings illustrate the exceptional accuracy of both NN^{F32} and NN^{F64}, as is evident for the out-of-sample errors as well as for the harmonic frequencies for H₂CO. As was demonstrated, if higher-order numerical derivatives are required for the target observable, *e.g.*, anharmonic frequencies based on perturbative approaches such as VPT2 or corrections to tunneling splittings, “roughness” of the PES originating from reduced (single) precision calculations deteriorate the performance (for VPT2 frequencies) or make computations entirely meaningless (correction to tunneling splittings). On the other hand, “roughness” of a magnitude found in the present work ($\sim 10^{-5}$ kcal/mol) appears to be inconsequential for MD simulations which only require first derivatives.

Acknowledgment

Support by the Swiss National Science Foundation through grants 200021_117810, 200021_215088, the NCCR MUST (to MM), and the University of Basel is acknowledged. This work was also partly supported by the United State Department of the Air Force, which is gratefully acknowledged (to MM). The authors thank Prof. J. O. Richardson and Dr. J. E. Lawrence for sharing computer codes to carry out the perturbative corrections and for discussions.

Data Availability Statement

The PhysNet Codes are available from <https://github.com/MMunibas/PhysNet>, the H₂CO data set is accessible at <https://zenodo.org/records/4585449> and the MP2 level data for

malonaldehyde can be found at <https://github.com/MMunibas/beta-diketones>.

References

- (1) LeCun, Y.; Cortes, C. MNIST handwritten digit database. 2010. URL <http://yann.lecun.com/exdb/mnist> **2010**, 7, 6.
- (2) Krizhevsky, A.; Hinton, G. Learning multiple layers of features from tiny images. *Computer Science Department, Univ. Toronto, Tech. Rep.* **2009**, 1.
- (3) Gupta, S.; Agrawal, A.; Gopalakrishnan, K.; Narayanan, P. Deep learning with limited numerical precision. International conference on machine learning. 2015; pp 1737–1746.
- (4) Wang, N.; Choi, J.; Brand, D.; Chen, C.-Y.; Gopalakrishnan, K. Training deep neural networks with 8-bit floating point numbers. *Adv. Neural Inf. Process.* **2018**, 31, 7675–7684.
- (5) Peng, H.; Wu, K.; Wei, Y.; Zhao, G.; Yang, Y.; Liu, Z.; Xiong, Y.; Yang, Z.; Ni, B.; Hu, J. FP8-LM: Training FP8 Large Language Models. *arXiv preprint arXiv:2310.18313* **2023**,
- (6) Micikevicius, P.; Stosic, D.; Burgess, N.; Cornea, M.; Dubey, P.; Grisenthwaite, R.; Ha, S.; Heinecke, A.; Judd, P.; Kamalu, J. FP8 formats for deep learning. *arXiv preprint arXiv:2209.05433* **2022**,
- (7) Manzhos, S.; Carrington Jr, T. Neural network potential energy surfaces for small molecules and reactions. *Chem. Rev.* **2020**, 121, 10187–10217.
- (8) Jiang, B.; Li, J.; Guo, H. High-fidelity potential energy surfaces for gas-phase and gas-surface scattering processes from machine learning. *J. Phys. Chem. Lett.* **2020**, 11, 5120–5131.

- (9) Unke, O. T.; Chmiela, S.; Sauceda, H. E.; Gastegger, M.; Poltavsky, I.; Schütt, K. T.; Tkatchenko, A.; Müller, K.-R. Machine learning force fields. *Chem. Rev.* **2021**, *121*, 10142–10186.
- (10) Meuwly, M. Machine learning for chemical reactions. *Chem. Rev.* **2021**, *121*, 10218–10239.
- (11) Käser, S.; Vazquez-Salazar, L. I.; Meuwly, M.; Töpfer, K. Neural network potentials for chemistry: concepts, applications and prospects. *Digital Discovery* **2023**, *2*, 28–58.
- (12) Unke, O. T.; Meuwly, M. PhysNet: A neural network for predicting energies, forces, dipole moments, and partial charges. *J. Chem. Theory Comput.* **2019**, *15*, 3678–3693.
- (13) Käser, S.; Boittier, E. D.; Upadhyay, M.; Meuwly, M. Transfer Learning to CCSD(T): Accurate Anharmonic Frequencies from Machine Learning Models. *J. Chem. Theory Comput.* **2021**, *17*, 3687–3699.
- (14) Smith, J. S.; Isayev, O.; Roitberg, A. E. ANI-1, A data set of 20 million calculated off-equilibrium conformations for organic molecules. *Sci. Data* **2017**, *4*, 1–8.
- (15) Kingma, D. P.; Ba, J. Adam: A method for stochastic optimization. *arXiv preprint arXiv:1412.6980* **2014**,
- (16) Käser, S.; Richardson, J. O.; Meuwly, M. Transfer Learning for Affordable and High-Quality Tunneling Splittings from Instanton Calculations. *J. Chem. Theory Comput.* **2022**, *18*, 6840–6850.
- (17) Barone, V. Anharmonic vibrational properties by a fully automated second-order perturbative approach. *J. Chem. Phys.* **2005**, *122*, 014108.
- (18) Antonio, P. D.; Lasalvia, M.; Perna, G.; Capozzi, V. Scale-independent roughness value of cell membranes studied by means of AFM technique. *Biochim. Biophys. Acta - Biomembr.* **2012**, *1818*, 3141–3148.

- (19) Bellitto, V. *Atomic force microscopy: imaging, measuring and manipulating surfaces at the atomic scale*; BoD–Books on Demand, 2012.
- (20) Richardson, J. O. Perspective: Ring-polymer instanton theory. *J. Chem. Phys.* **2018**, *148*, 200901.
- (21) Firth, D.; Beyer, K.; Dvorak, M.; Reeve, S.; Grushow, A.; Leopold, K. Tunable far-infrared spectroscopy of malonaldehyde. *J. Chem. Phys.* **1991**, *94*, 1812–1819.
- (22) Wang, Y.; Braams, B. J.; Bowman, J. M.; Carter, S.; Tew, D. P. Full-dimensional quantum calculations of ground-state tunneling splitting of malonaldehyde using an accurate ab initio potential energy surface. *J. Chem. Phys.* **2008**, *128*, 224314.
- (23) Jahr, E.; Laude, G.; Richardson, J. O. Instanton theory of tunneling in molecules with asymmetric isotopic substitutions. *J. Chem. Phys.* **2020**, *153*, 094101.
- (24) Baba, T.; Tanaka, T.; Morino, I.; Yamada, K. M.; Tanaka, K. Detection of the tunneling-rotation transitions of malonaldehyde in the submillimeter-wave region. *J. Chem. Phys.* **1999**, *110*, 4131–4133.
- (25) Lawrence, J. E.; Dušek, J.; Richardson, J. O. Perturbatively corrected ring-polymer instanton theory for accurate tunneling splittings. *J. Chem. Phys.* **2023**, *159*.
- (26) Mizukami, W.; Habershon, S.; Tew, D. P. A compact and accurate semi-global potential energy surface for malonaldehyde from constrained least squares regression. *J. Chem. Phys.* **2014**, *141*.
- (27) Verlet, L. Computer” experiments” on classical fluids. I. Thermodynamical properties of Lennard-Jones molecules. *Phys. Rev.* **1967**, *159*, 98.
- (28) Larsen, A. H. et al. The atomic simulation environment—a Python library for working with atoms. *J. Phys. Condens. Matter.* **2017**, *29*, 273002.

- (29) Käser, S.; Unke, O. T.; Meuwly, M. Isomerization and decomposition reactions of acetaldehyde relevant to atmospheric processes from dynamics simulations on neural network-based potential energy surfaces. *J. Chem. Phys.* **2020**, *152*, 214304.
- (30) Chmiela, S.; Vassilev-Galindo, V.; Unke, O. T.; Kabylda, A.; Saucedo, H. E.; Tkatchenko, A.; Müller, K.-R. Accurate global machine learning force fields for molecules with hundreds of atoms. *Sci. Adv.* **2023**, *9*, eadf0873.
- (31) Upadhyay, M.; Meuwly, M. Thermal and Vibrationally Activated Decomposition of the syn-CH₃CHOO Criegee Intermediate. *ACS Earth Space Chem.* **2021**, *5*, 3396–3406.
- (32) Lippert, R. A.; Bowers, K. J.; Dror, R. O.; Eastwood, M. P.; Gregersen, B. A.; Klepeis, J. L.; Kolossvary, I.; Shaw, D. E. A common, avoidable source of error in molecular dynamics integrators. *J. Chem. Phys.* **2007**, *126*, 046101.
- (33) Schütz, M.; Hetzer, G.; Werner, H.-J. Low-order scaling local electron correlation methods. I. Linear scaling local MP2. *J. Chem. Phys.* **1999**, *111*, 5691–5705.
- (34) Wang, Z.; Aldossary, A.; Shi, T.; Liu, Y.; Li, X. S.; Head-Gordon, M. Local Second-Order Møller–Plesset Theory with a Single Threshold Using Orthogonal Virtual Orbitals: Theory, Implementation, and Assessment. *J. Chem. Theory Comput.* **2023**, *19*, 7577–7591.